Carbon nanotube electronics / Électronique à nanotubes de carbone

Carbon nanotube chemistry and assembly for electronic devices

Vincent Derycke [a,*], Stéphane Auvray [a], Julien Borghetti [a], Chia-Ling Chung [a],
Roland Lefèvre [a], Alejandro Lopez-Bezanilla [b], Khoa Nguyen [a], Gaël Robert [a],
Gregory Schmidt [a], Costin Anghel [a], Nicolas Chimot [a], Sébastien Lyonnais [a],
Stéphane Streiff [a], Stéphane Campidelli [a], Pascale Chenevier [a], Arianna Filoramo [a],
Marcelo F. Goffman [a], Laurence Goux-Capes [a], Sylvain Latil [c], Xavier Blase [d],
François Triozon [e], Stephan Roche [b], Jean-Philippe Bourgoin [a]

[a] *Laboratoire d'Électronique Moléculaire, Service de Physique de l'État Condensé (CNRS URA 2464), CEA, IRAMIS,
91191 Gif-sur-Yvette, France*
[b] *SPSMS, CEA, INAC, 17, avenue des Martyrs, 38054 Grenoble, France*
[c] *Service de Physique et Chimie des Surfaces et Interfaces, CEA, IRAMIS, 91191 Gif-sur-Yvette, France*
[d] *Institut Néel, CNRS and université Joseph-Fourier, BP 166, 38042 Grenoble cedex 9, France*
[e] *CEA, LETI, MINATEC, 38054 Grenoble, France*

Abstract

Carbon nanotubes (CNTs) have exceptional physical properties that make them one of the most promising building blocks for future nanotechnologies. They may in particular play an important role in the development of innovative electronic devices in the fields of flexible electronics, ultra-high sensitivity sensors, high frequency electronics, opto-electronics, energy sources and nano-electromechanical systems (NEMS). Proofs of concept of several high performance devices already exist, usually at the single device level, but there remain many serious scientific issues to be solved before the viability of such routes can be evaluated. In particular, the main concern regards the controlled synthesis and positioning of nanotubes. In our opinion, truly innovative use of these nano-objects will come from: (i) the combination of some of their complementary physical properties, such as combining their electrical and mechanical properties; (ii) the combination of their properties with additional benefits coming from other molecules grafted on the nanotubes (this route being particularly relevant for gas- and bio-sensors, opto-electronic devices and energy sources); and (iii) the use of chemically- or bio-directed self-assembly processes to allow the efficient combination of several devices into functional arrays or circuits. In this article, we review our recent results concerning nanotube chemistry and assembly and their use to develop electronic devices. In particular, we present carbon nanotube field effect transistors and their chemical optimization, high frequency nanotube transistors, nanotube-based opto-electronic devices with memory capabilities and nanotube-based nano-electromechanical systems (NEMS). The impact of chemical functionalization on the electronic properties of CNTs is analyzed on the basis of theoretical calculations. ***To cite this article: V. Derycke et al., C. R. Physique 10 (2009).***
© 2009 Académie des sciences. Published by Elsevier Masson SAS. All rights reserved.

Résumé

Fonctionnalisation chimique et assemblage des nanotubes de carbone pour l'électronique. Les nanotubes de carbone (CNTs) ont des propriétés physiques exceptionnelles qui en font l'une des briques de base les plus prometteuses des nanotech-

---

* Corresponding author.
  E-mail address: vincent.derycke@cea.fr (V. Derycke).

nologies. En particulier, ils peuvent jouer un rôle important pour le développement de composants électroniques innovants dans les domaines de l'électronique flexible, des détecteurs ultra-sensibles, de l'électronique haute fréquence, de l'optoélectronique, des sources d'énergie et des systèmes nano-électromécaniques (NEMS). Des démonstrations de faisabilité ont été réalisées, souvent à l'échelle du composant individuel, mais il reste de nombreux verrous à lever avant que ne puisse être évaluée la viabilité de ces composants. Le contrôle de la synthèse et celui du positionnement sont notamment critiques. Nous pensons que l'utilisation réellement innovante de ces nano-objets peut venir de (i) la combinaison de plusieurs de leurs propriétés (électriques et mécaniques par exemple) ; (ii) la combinaison de leurs propriétés avec les bénéfices additionnels apportés par d'autres molécules greffées sur les nanotubes (cette voie est particulièrement pertinente pour les détecteurs de gaz, les détecteurs de molécules biologiques, l'optoélectronique et les sources d'énergie) ; et (iii) l'utilisation de méthodes d'auto-assemblage chimiques ou bio-dirigées permettant de combiner les dispositifs en circuits. Dans cet article, nous présentons une revue de nos travaux récents concernant la chimie et l'assemblage des nanotubes et leur utilisation pour le développement de dispositifs électroniques. En particulier, nous présentons des transistors à nanotubes de carbone et leur optimisation par voie chimique, des transistors haute fréquence, des composants optoélectroniques fonctionnant comme des mémoires et des composants nano-électromécaniques. L'impact de la fonctionnalisation chimique sur les propriétés électroniques des CNTs est analysé sur la base d'études théoriques. ***Pour citer cet article : V. Derycke et al., C. R. Physique 10 (2009).***

1. Introduction

While the different allotropic forms of carbon (diamond, graphite, graphene, C_{60} molecule etc.) refer to well defined structures, the name 'carbon nanotube' (CNT) encompasses a large variety of different objects, which differ from each other in terms of diameter, length, chirality, electronic properties and number of shells in the case of multi-wall nanotubes (MWNTs). It can be a chance for future applications since different types of nanotubes can be better suited for different types of use. For example, the mechanical properties of multi-wall nanotubes with intermediate diameter (5–15 nm) are of particular interest in the field of NEMS. Semiconducting single-wall nanotubes (SWNTs) can serve as channel in field effect transistors, while metallic SWNTs could be important as nanoscale interconnects or nanoscale electrodes. The counterpart of this diversity is the difficulty to obtain and study well-defined objects of homogeneous composition and properties.

There are principally two classes of synthesis methods for carbon nanotubes: high temperature methods (such as arc discharge and laser ablation) and chemical vapor deposition (CVD) methods. From an electronic device point of view, they are also referred to as *ex situ* and *in situ* methods. Indeed, in the first case, carbon nanotubes are prepared in a first step and later deposited onto the substrate on which electronic devices are to be built. In the second case, nanotubes are directly grown on silicon (or quartz) wafers at the location where they will be used, by the pre-synthesis localization of the growth catalyst. This second method has interesting advantages but suffers from the critical difficulty of growing nanotubes of homogeneous type. If the CVD growth of single-wall nanotubes with a very narrow diameter distribution is now well mastered, it is still impossible to control the precise chirality, which results in the mixed synthesis of both metallic and semiconducting SWNTs. The *ex situ* methods offer other types of interesting advantages especially from a chemistry point of view. Indeed, since these nanotubes are handled in solution, they can be chemically functionalized [1] and are compatible with several emerging techniques to separate metallic and semiconducting nanotubes [2]. Moreover, the use of these nanotubes can be combined with different chemical or bio-directed self-assembly techniques so as to place them at required locations in a device or a circuit.

In this article, we present our strategy to build and study electronic devices starting from commercial nanotubes and going through different steps of chemical purification [3,4], solubilization, functionalization [4,5] and assembly [6–12]. We think that these steps are the key to the development of innovative electronic functions. In particular, we studied carbon nanotube field effect transistors and their chemical optimization [13,14], high frequency nanotube transistors [15–17], nanotube-based opto-electronic devices with memory capabilities [18,19] and nanotube-based nano-electromechanical systems (NEMS) [20,21]. An important issue associated with the manipulation of nanotubes in solution and their functionalization relates to the impact of chemical modifications on their transport properties. In this article, we present theoretical results that address this critical issue [22].

2. Nanotube solubilization, purification and functionalization

SWNTs from *ex situ* growth methods are produced in soot containing a large proportion of metal particles used as growth catalysts and amorphous carbon particles. Metal particles can be embedded in carbon shells issued from the growth and are usually linked to SWNTs. Besides, carbon particles and carbon nanotubes are both constituted of sp^2 carbon with similar chemical reactivity. Therefore the purification conditions have to be fine tuned to selectively etch amorphous carbon while preserving the carbon nanotube structure. The carbon nanotube reactivity strongly depends on their diameter, the smaller diameter SWNTs being far more reactive because of their higher curvature, so that purification conditions have to be adapted to each SWNT source according to the average nanotube diameter.

Among the different types of CNTs that can be handled in solution, laser ablation and arc discharge SWNTs are preferred in molecular electronics because their high crystalline quality provides good electrical characteristics. Typically, these SWNTs can be isolated from the raw soot using a classical nitric acid treatment optimized for our purposes [3,4]. First, SWNTs are boiled for 4 h in nitric acid aqueous solution (35%) to oxidize amorphous carbon and metal catalysts. After the acid is rinsed out, treatment in boiling 30% hydrogen peroxide finishes cleaning the nanotubes and removing amorphous carbon. Alternatively, simply rinsing the nitric acid treated nanotubes with a mildly alkaline aqueous solution (1 mM NaOH) dissolves most of the already partially etched amorphous carbon particles while the SWNTs remain insoluble. Purified SWNTs are recovered by filtration. A typical absorption spectrum is shown in black in Fig. 1(a). Following such purification, separation of SWNTs according to length can be performed. For that purpose, purified SWNTs are dissolved in aqueous solution using poloxamer F127 as a surfactant and separated using size exclusion chromatography (SEC) [4]. SWNTs are sorted according to length, from 1 to 3 µm length in the first fractions to less than 100 nm in the last fractions. The sharp absorption spectra and AFM images (Fig. 1) of the SEC purified SWNTs indicates, in particular, the absence of small particles that are collected in a separate fraction. Interestingly SEC fraction absorption spectra show a slight enrichment in large diameter SWNTs in the first (long CNTs) fractions while small diameter SWNTs are more concentrated in the last (short CNTs), as expected from the higher sensitivity of smaller diameter SWNTs to chemical etching.

Along with the wide spread use of SWNTs in devices, SWNT functionalization methods have flourished to help in processing this highly insoluble material, as well as to add new functionalities such as tuned light absorption or chemical sensing. Among the covalent functionalization methods, diazonium to SWNTs coupling is the most wide-spread because of its handiness and high yield. Nevertheless, the mechanism of this complex reaction remained mysterious. Using chemical kinetics methods, we thoroughly studied the mechanism of the reaction, aiming at better mastering the coupling rate and at controlling the selectivity of the reaction towards metallic SWNTs. Chemical kinetics as well as electron spin resonance demonstrated without ambiguity a free radical chain reaction involving SWNT stable radicals [4]. In the propagation phase, the aryl radical reacts with SWNT to yield an aryl-SWNT radical, then the aryl-SWNT radical reduces the aryl diazonium into a new aryl radical. The origin of the selectivity of the reaction towards metallic SWNTs was unveiled. Indeed, metallic SWNTs have a higher HOMO (Higher Occupied Molecular Orbital) than semiconducting SWNTs, which enhances their reactivity towards the electrophilic aryl radical.

Nanotubes by themselves already combine many exceptional physical properties. Still, both the development of new functionalities for individual devices and the assembly of complex structures and circuits could be improved by the incorporation of highly engineered molecules on the nanotube surfaces. There is thus a real need for simple and versatile procedures which allow the introduction of new functional groups onto the nanotube surface. In particular, we recently investigated the functionalization of SWNTs with Zn-phthalocyanine derivatives *via* "click chemistry" and demonstrated that this concept can be used for the realization of photovoltaic cells [5]. The term "click chemistry" [23] defines a series of clean, versatile, specific chemical reactions, easy to realize and exhibiting simple purification process (absence of by-products). Among the large collection of organic reactions, *Huisgen* cycloaddition (1,3-dipolar cycloaddition between azide and acetylene derivatives in the presence of Cu(I) catalyst) represents the most effective reaction of the "click chemistry" [24–27]. It has been demonstrated that the emerging field of "click chemistry" can bring very elegant solutions to easily achieve nanotube-based functional materials [5,28,29]. In our recent experiments, we described the functionalization of single-wall carbon nanotubes (SWNTs) with 4-(2-trimethylsilyl)ethynylaniline and the subsequent attachment of a zinc-phthalocyanine (ZnPc) derivative using the reliable Huisgen 1,3-dipolar cycloaddition (Fig. 2). The SWNT-ZnPc nanoconjugate was fully characterized and a photoinduced communication between the two photoactive components (i.e., SWNT and ZnPc) was identified. Such beneficial features led us to incorporate the SWNT-ZnPc hybrid in a photoelectrochemical cell as photoactive material in an ITO photoanode.
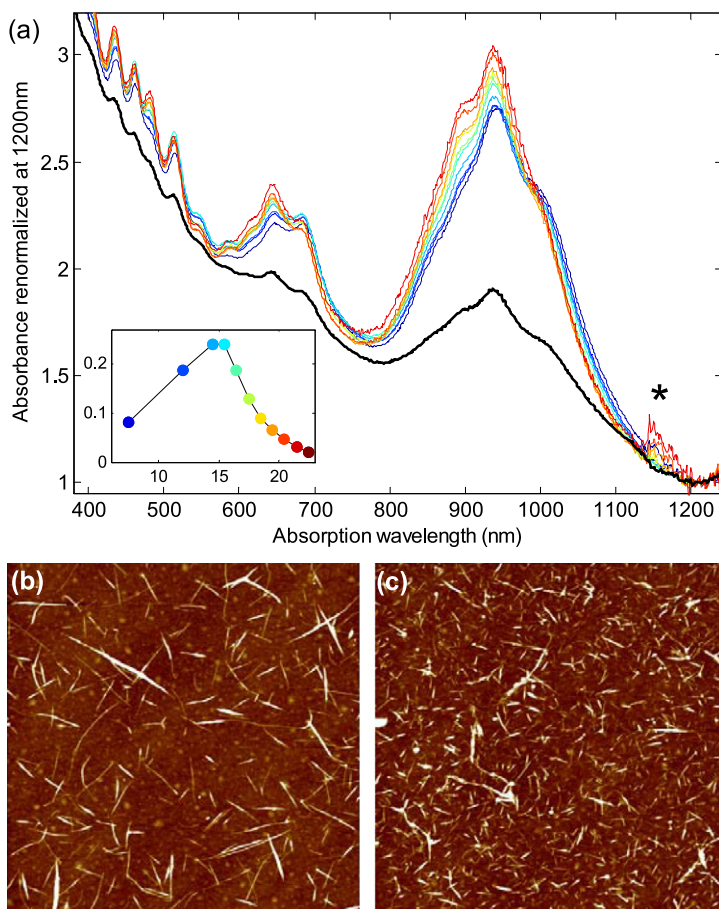
Fig. 1. (a) Absorption spectra of successive SEC (size exclusion chromatography) fractions of arc discharge SWNTs in 2% F127 aqueous solution on Sephacryl S500. The fraction spectra are plotted in rainbow color from blue (long CNTs) to red (short CNTs), while the initial solution spectrum is plotted in black. Absorbance spectra have been normalized at 1200 nm to allow for comparison. The peak labeled with a star is an artifact due to water absorption subtraction. Inset: absorbance at 1200 nm for each fraction as a function of elution volume (mL), which indicates the relative concentration of each length fractions. (b), (c) AFM image 5×5 μm^2 of two fractions corresponding to long and short CNTs respectively.

The use of such hybrid CNT-molecule objects is also studied in our laboratory in the context of optically controlled nanotube transistors.

3. Impact of chemical functionalization on the transport properties of SWNTs

Chemical functionalization is recognized as a very efficient way of tuning the electronic properties of CNTs, allowing new device functionality. In particular in the field of bio- and chemical sensors, functionalization may lead to the specific detection of single molecule binding events [30]. In optoelectronics, the grafting of photo-sensitive molecules onto the nanotube sidewalls allows building optically controlled nanotube-based devices [31,32], for example.

In practice, both physisorption and chemisorption provide effective pathways for modifying the intrinsic properties of CNTs. However, it is not clear at the moment which method yields the better compromise between the improvement of the targeted functionality and the degradation of the nanotube conductivity upon functionalization [33]. In the case of physisorption, the scattering resulting from molecule deposition over the nanotube surface is vanishingly low due to the weak amount of charge transferred between both systems [34]. Non-covalent adsorption has therefore the advantage of enabling CNTs functionalization while still preserving their electronic structure. Indeed, the original sp^2 hybridized bondings and aromaticity remain unaltered [35]. In contrast, covalent functionalization of CNTs involves the formation of saturated sp^3 bonds which break the p_z network symmetry of the nanotube surface [36]. The
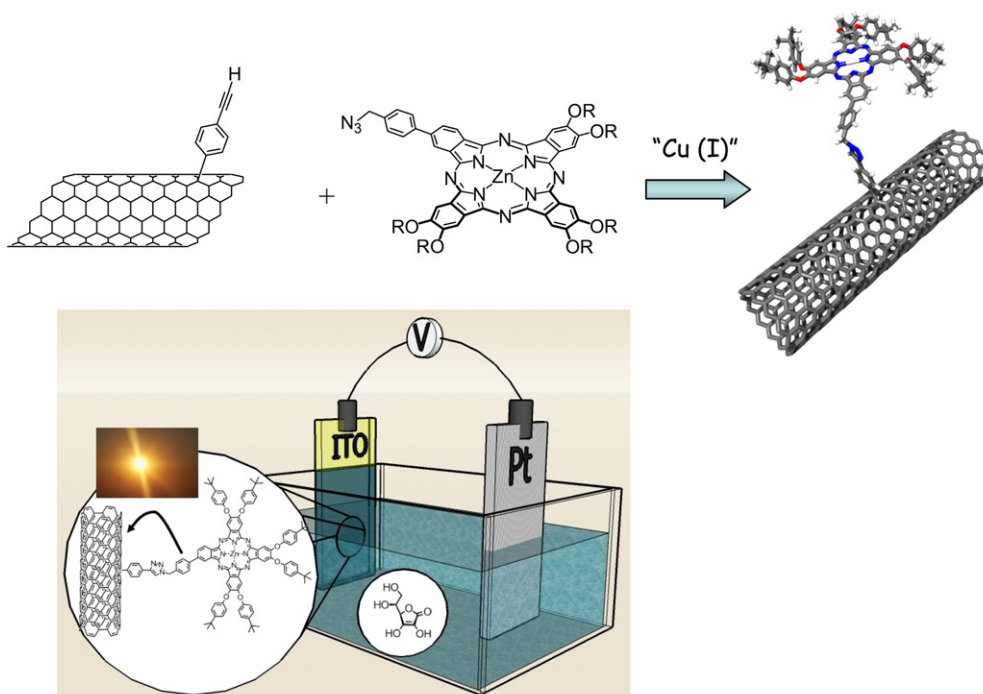
Fig. 2. Principle of the addition of phthalocyanine on SWNTs via "click chemistry" and schematic representation of the photoelectrochemical cell containing the SWNT-ZnPc conjugate [5].

consequence is a dramatic loss in charge transport ability [37,38]. Rehybridization introduces resonant states in the electronic structure of the pristine CNT which act as scattering centres. This particular difference on the electrochemical nature of the bonding turns out to be critical for the preservation of good transport properties over large distances. The impact of covalent functionalization on the tube conductance can, however, be significantly reduced by a suitable choice of the addends. Using *ab initio* calculations, we have recently reported [22] indications that cycloaddition reactions leading to the grafting of carbene groups (CH_2) could preserve most of the conductance of 1 μm (6, 6) and (10, 10) metallic CNTs, in contrast to phenyl-type functionalization that would result in strong damping of conduction ability.

As an example, we present here a computational study of electronic transport properties in metallic SWNTs with random distribution of carbene or phenyl functional groups strongly bonded to the nanotube sidewalls. An efficient numerical method based on *ab initio* density functional theory has been used. First principles calculations are initially performed to obtain the self-consistent *ab initio* Hamiltonian and overlap matrix of a building block composed of a CNT with the corresponding grafted functional groups. The Hamiltonian obtained after structural atomic relaxation is further implemented into a transport calculation and, by assembling the building blocks in an aperiodic fashion, realistically long and disordered systems can be investigated. The quantum transport modelling is based on a conventional Green's function formalism, combining an iterative scheme for the calculation of transmission coefficients with the Landauer–Büttiker formula for the coherent conductance [39]. The conductance changes from quasiballistic to diffusive conduction regime depending on the attached molecule. Fig. 3 shows the computed conductance signature of functionalized metallic nanotubes as a function of both incident electron energy and tube diameter, for a fixed coverage density. The conduction is clearly more strongly disrupted in the case of phenyls when compared with carbene functionalization. We also observe the complete suppression of conductance for the (6, 6) tube in contrast to the (10, 10) that still shows some transport capability for the same number of attached molecules. The reduction of disorder when increasing the nanotube diameter stems from a reduction of the scattering probability. In contrast, grafted carbene molecules poorly affect the nanotube conductance, especially in the first plateau, with a slight conductance asymmetry with respect to the charge neutrality point. The results evidence the robustness of quasiballistic conduction in case of carbene cycloadditions for long carbon nanotubes, as also discussed by Marzari and coworkers [40,41]. This
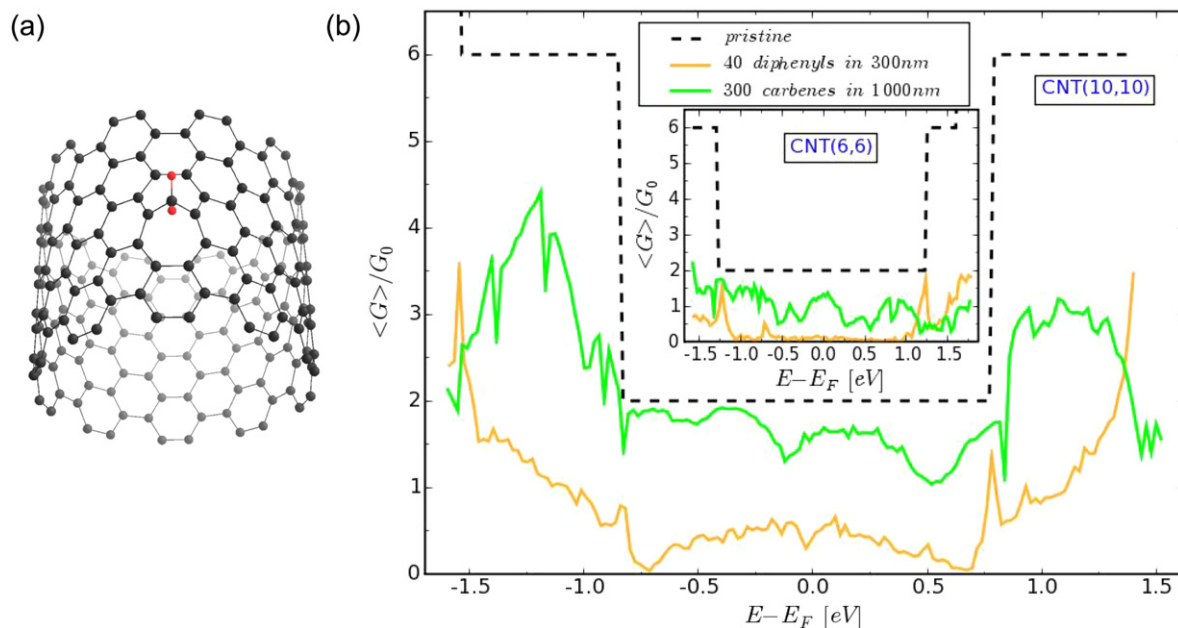
(a) (b)

Fig. 3. (a) Atomic structure of a portion of SWNTs after covalent addition of a single carbene group CH_2. (b) Average of the transmission as a function of energy in the case of 1000 nm and 300 nm long (10, 10) CNTs respectively functionalized with CH_2 (green) and pairs of phenyl groups (yellow). Insert: same for a (6, 6) CNT. The dashed lines show the transmission for a pristine CNT.

demonstrates the non-invasive character of carbene functionalization which preserves good conduction capabilities of armchair nanotubes, and suggests this type of functionalization as a better option for adding new functionalities to nanotube-based devices.

4. Selective placement of nanotubes

To fully take advantage of the unique electrical properties of SWNTs in device/circuit applications, it is necessary to be able to selectively place them at specific locations on a substrate with a low cost and high yield technique, preferentially based on self-assembly. Depending on the type of nanotubes (SWNTs, MWNTs) and the type of study, different configurations of deposited nanotubes are required. It ranges from individual, supported or suspended, nanotubes to large networks of randomly oriented or aligned nanotubes. The placement method should thus be adapted to particular experiments. We preferentially use three different techniques of selective deposition: (i) chemically-assisted self-assembly on patterned molecular monolayers, (ii) dielectrophoresis and (iii) bio-directed self-assembly.

Since 2000 we have developed and optimized a technique of localized nanotube deposition assisted by self-assembled monolayers (SAMs). The approach is based on the grafting of amine terminated SAMs to modify the surface properties of certain regions of a SiO_2 substrate. This affects the interactions between the sidewalls of CNTs and the surface so that the CNTs in solution are preferentially captured on the pattern. This kind of studies started with the pioneering works of Liu et al. [42], Muster et al. [43] and Choi et al. [6]. The combination of adapted organic solvent and well organized monolayers allowed us to control both the deposition density and selectivity [7–9]. The process can be summarized as follows: electron-beam lithography is performed on PMMA deposited on the SiO_2 surface of a Si substrate. After a cleaning step, a monolayer of aminopropyltriethoxysilane (APTS) is deposited to form a "sticky patch" in regions opened in the resist. Exposure to Ethylenediamine (EDA) is used to increase the surface concentration and the orientation of APTS and consequently to improve interactions with SWNTs. The gas deposition was favoured instead of silanisation from an aqueous solution since it yields a much better control of the layer thickness. Once the sticky patch has been formed the adhesion of CNTs is enhanced in the functionalized regions. We first used aqueous solution of CNTs and in this case the sample was first exposed to the SWNTs suspension and then the resist was lifted off. However, to improve the dispersion of SWNTs in the solution and increase the density of the deposition, the use of an organic solvent is preferable. We use N-Methyl Pyrrolidone (NMP) and perform the lift-off
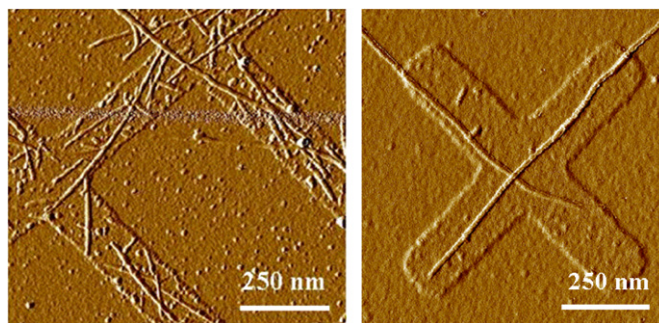
Fig. 4. AFM images showing the efficiency of the APTS-assisted selective deposition technique. Patterned areas of a Si/SiO$_2$ wafer grafted with a monolayer of APTS act as 'sticky patches' for the localized adsorption of SWNTs from solution.

of the resist before the nanotube deposition. Fig. 4 shows that this method leads to the deposition of CNTs exclusively on defined areas and that both high density and individual CNTs can be obtained by adjusting the deposition protocol. From a device point of view, we efficiently used this technique to build field-effect transistors based on individual SWNTs [14,18] or network of CNTs [15] and electromechanical switches based on individual MWNTs [21].

A second deposition technique which is of particular interest for carbon nanotubes is dielectrophoresis (DEP) [44]. It consists in depositing a droplet of a nanotube solution (in an organic solvent or in water with surfactant) on pre-patterned electrodes and applying between these electrodes an AC electric field in the MHz range. The polarisability of carbon nanotubes induces an increase in nanotube concentration in the area of high electric field and the favourable alignment of the nanotubes along the field lines. As shown in Fig. 5(a)–(c) the method works for both MWNTs and SWNTs, and for both individual and dense networks of nanotubes. As will be described in the device sections below, such individual MWNT can be incorporated in NEMS, while dense nanotube networks are important for the development of high frequency devices. In both cases, alignment of the CNTs respective to predefined structures is crucial. A particularity of the DEP technique is that, due to their higher dielectric constant, metallic nanotubes are more favourably attracted and deposited. It can be seen as a drawback for the fabrication of nanotube field effect transistors but it can also be used as a way to separate metallic from semiconducting CNTs [44]. An illustration of such selectivity is presented in Fig. 5(d). We prepare a set of electrodes, cover them with a CNT solution droplet of low concentration and perform a series of DEP depositions. The different sets of electrodes are then used as source–drain electrodes in an FET configuration (with the back-side of the SiO$_2$-covered Si wafer serving as gate electrode). The first deposition steps progressively remove most of the metallic nanotubes from the solution so that the last prepared devices contain mainly semiconducting nanotubes, corresponding to lower on-current but much higher on-off ratio (defined as the ratio between the current at negative gate bias and at positive gate bias for such p-type transistors). For the large scale production of devices incorporating only one type of SWNTs (metallic or semiconducting), using solutions of sorted CNTs is of course more efficient. Still, this simple method proves very useful to study, for example, the specific reactivity of the two types of CNTs with respect to chemical treatments.

Because of its unique recognition properties, its size and the sub-nanometric resolution, DNA is of particular interest for positioning and organizing nanomaterials, and in particular SWNTs. Moreover, in DNA-directed na-noelectronics, DNA can be envisioned not only as a positioning scaffold, but also as a support for the conducting elements [45,46]. With the aim of fabricating carbon nanotube-based devices by combining DNA with SWNTs, we studied two complementary strategies (Fig. 6): the covalent linkage of DNA on carboxylic groups of SWNTs under classical coupling conditions [10] and the non-covalent approach based on biotin-streptavidin molecular recognition properties [10–12]. The main advantage of the covalent approach is that the linkage can be favoured at the end of the CNTs (Fig. 6(c)). In the initial step of the reaction, a mild acid treatment results in the formation of carboxylic groups both along the nanotubes and at their end. But the use of an adapted surfactant act as a protecting layer for the reactive group along the CNT walls so that end-bonding is mainly obtained. Still, this covalent approach has a limited yield and may affect the conducting properties of the CNTs. The non-covalent approach can achieve a higher yield and preserve the structural quality of the CNTs. In addition, complex structures can be fabricated by DNA strands engineering. For example, we incorporated biotin at tagged locations along DNA molecules [11] or close to the intersection site of
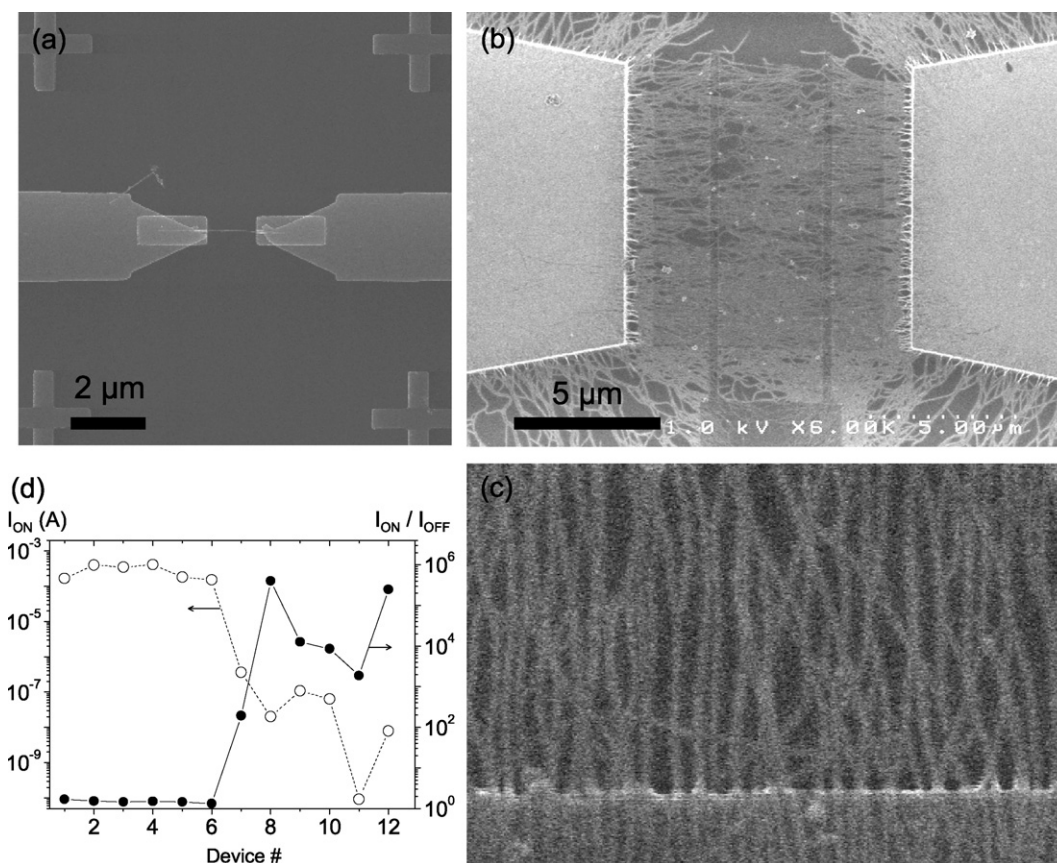
Fig. 5. Scanning electron microscopy (SEM) images of: (a) An individual MWNT selectively deposited by DEP from solution on predefined electrodes (and then re-contacted). (b) A dense network of SWNTs deposited by DEP between macroscopic electrodes and over a two-finger Al/AlO$_x$ back-gate electrode. This design is the one used (after source and drain contact fabrication) for the study of high frequency CNT transistors as described in the device section [16]. (c) Higher magnification image showing the high degree of alignment of SWNTs deposited by DEP. (d) On-current and I_{ON}/I_{OFF} ratio of CNT network transistors built from SWNTs deposited by DEP from the same droplet of solution. The first deposited CNTs are predominantly metallic (high current, no gate modulation). After most of the metallic SWNTs have been removed from the solution, the deposited SWNTs become dominant.

T-shape DNA structures [12]. Such synthesis of three branch DNA scaffolds and the insertion of CNTs at their centre are the first steps toward the bio-directed self-assembly of nanotube transistors with individual gates.

Once DNA-CNT hybrid objects have been prepared and deposited (ideally using DNA hybridization to guide the assembly), the DNA scaffold can be transformed into an interconnecting network by selective metallization of the DNA strands [45,46]. To turn DNA into conducting leads, we developed a novel approach for DNA metallization [47]. The progressive growth of nanowires was achieved by the slow and selective precipitation of palladium oxide on DNA molecules previously deposited on a dry substrate (Fig. 7). The second step consisted on the reduction of the palladium oxide into metallic palladium. We fabricated homogeneous, continuous and conductive DNA-based Pd nanowires with very thin diameter (20–25 nm). In addition, the method proposed is very selective as almost no parasitic metallization of the surface is obtained.

5. SWNT-based field effect transistors

Once carbon nanotubes have been purified, solubilized, possibly functionalized and finally deposited by one of the selective deposition or self-assembly methods, they can be connected in a device geometry which allows the study of their electronic properties. An interesting geometry for such studies is the field effect transistor, in which a semiconducting nanotube serves as the channel, the conductivity of which is controlled by a capacitively coupled gate
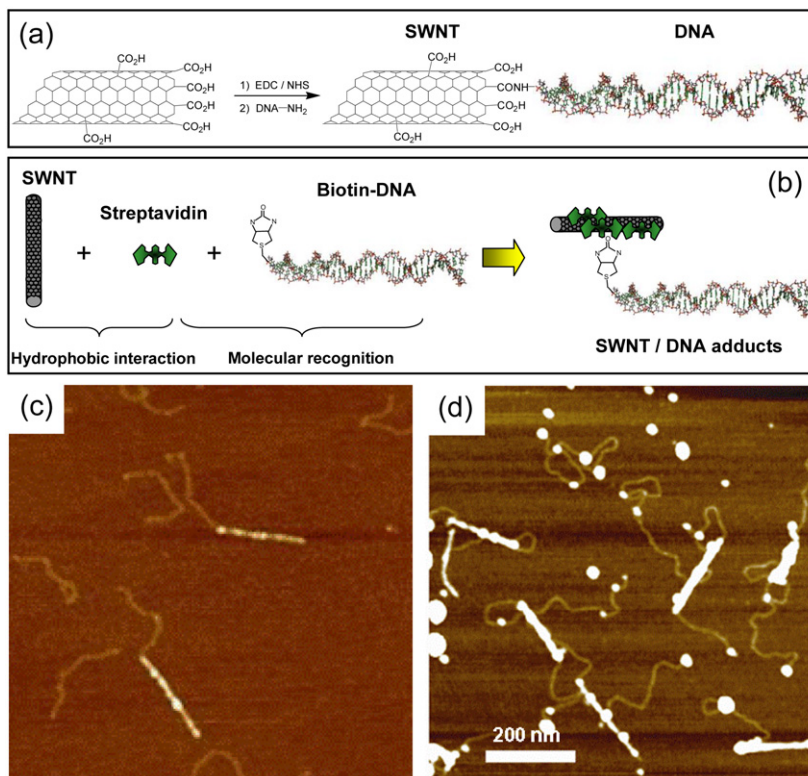
Fig. 6. (a) Principle of the covalent coupling of DNA to CNTs using the reaction of amine groups on DNA with acid carboxylic groups on CNTs in the presence of EDC and NHS. (b) Principle of the non-covalent coupling of DNA to CNTs using the streptavidin–biotin recognition capabilities. (c), (d) AFM images of CNT-DNA hybrids built by covalent (c) and non-covalent (d) coupling.

electrode [48,49]. Due to the exceptional electronic properties of carbon nanotubes [50] (in particular, the very long carrier mean free path, the high carrier velocity and the high current density capability), aggressively scaled carbon nanotube field effect transistors (CNTFETs) are among the best performing nano-scale FETs [51–54].

5.1. Chemical sensitivity of carbon nanotube transistors

An important particularity of these transistors is their high sensitivity to small modifications of their environment, which was proposed as a basis for the development of gas- and bio-sensors [55,56,30]. This sensitivity comes from the surface-only nature of the carbon atoms of the nanotube, from their molecular scale and from the specificity of the electrostatic in one-dimensional objects. Both accessing a high level of performances and improving/controlling the sensitivity of CNTFETs requires mastering the different interfaces at the molecular scale. These interfaces are: (i) the nanotube–electrode interface; (ii) the nanotube–dielectric interface; and (iii) the nanotube-wall–surrounding media (air, water, coating layer, . . .) interface.

Contacting a semiconducting SWNT by metallic electrodes leads to the formation of Schottky barriers of significant height at the metal–CNT interfaces (except in the case where palladium contacts are used together with nanotube diameter above 1.4 nm [57,58], in which case the barrier height is negligible). When the nanotube is short (<200–500 nm) and of sufficient quality, scattering along the nanotube is limited and quasi ballistic transport takes place [50,59]. In that case, the height of the Schottky barrier at the source contact and the coupling of its width to the gate potential are the principal factors determining the performance of the transistor. The nanotube–metal interface involving only a small number of atoms, the barrier height is extremely sensitive to very small changes of the environment and in particular to molecular adsorption [60]. In the recent years, we have worked on the chemical optimization of CNTFETs and showed that an appropriate chemical treatment of the source and drain electrodes can significantly improve holes injections at the nanotube–source electrode interface [13]. Indeed, assembling a molecular layer of ap-
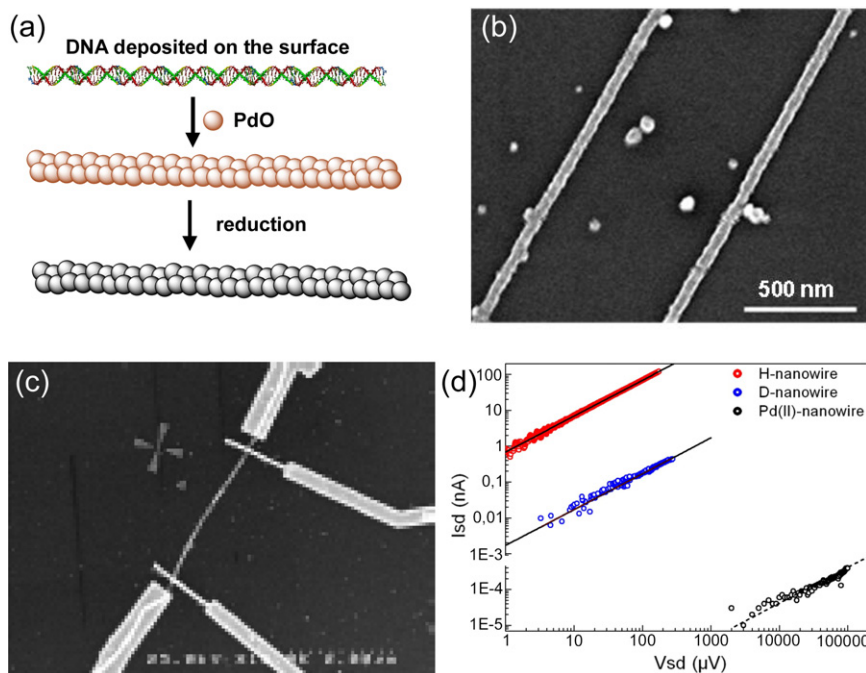
Fig. 7. (a) Schematic representation of Pd-based nanowires growth from DNA. (b), (c) SEM images of the nanowires obtained before (b) and after (c) post fabrication of electrodes by e-beam lithography. (d) Evolution of the conductivity of a Pd-nanowire before (black) and after reduction using DMAB (blue) or hydrogen (red) as reductor [47].
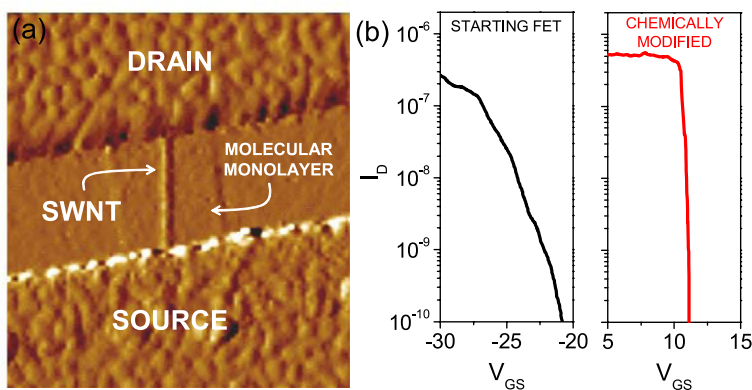

Fig. 8. AFM image (phase mode) of a carbon nanotube field-effect transistor fabricated by chemical self-assembly (source–drain separation 100 nm). (b) Effect on the transfer characteristics of the chemical treatment of the device by an acid in the gas phase. The effect comes from the cumulated actions of an improvement of holes injection at the source electrode and a doping by protonation of the amine terminated APTS surface used for the selective deposition process. $V_{DS} = -200$ mV.

propriate polar molecules on the gold source electrode leads to an increase of its effective work function thus reducing the Schottky barrier height at the metal-nanotube junction. As an example, we showed that exposing CNTFETs to vapors of trifluoro-acetic acid (TFA) decreases the subthreshold slope (a figure of merit known to be sensitive to the barrier height in CNTFETs [61]) of the transistor by a factor of ∼4.5 [13].

We then showed that a second interface can be put to profit to tune the electrical characteristics of CNTFETs: the nanotube–gate dielectric interface. In this case, our CNTFET fabrication technique involves a molecular monolayer of APTS grafted on the SiO₂ surface, as presented above. This layer allows the selective deposition of nanotubes exclusively on chemically modified patterns (see Fig. 8). By adjusting the charge on this layer using an acid or an
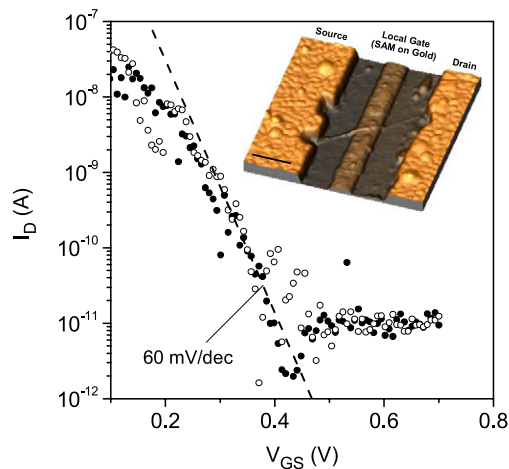
Fig. 9. Transfer characteristic $I_D(V_{GS})$ of a carbon nanotube transistor using a self-assembled molecular mono-layer of octadecanethiol on gold as ultra-thin gate dielectric ($V_{DS} = -100$ mV). The dotted line corresponds to the ideal 60 mV/dec subthreshold slope. Insert: AFM image illustrating the proposed device geometry.

alkaline gas, we can very efficiently modify the doping level of the transistor channel [14]. In particular, protonating the amine groups at the dielectric surface using TFA leads to a p-type doping, that combines with the effect of TFA on the efficiency of hole injection at the source contact, to yield a drastically improved transfer characteristics (Fig. 8). N-type doping was also obtained using triethylamine to inverse the charge at the CNT-SiO$_2$ interface. Notably, this experiment could also be used to demonstrate 10 ppb range detection sensitivity in the case of triethylamine [14].

In this experiment, the gate dielectric of the transistor is covered with a molecular layer but this layer barely affects the capacitive coupling between the gate and the CNT. Most of the CNTFETs reported in the literature were fabricated using inorganic dielectrics (SiO$_2$, Al$_2$O$_3$, HfO$_2$, ...). Recently, several groups proposed the use of organic or molecular [62,63] dielectrics. It is an interesting step toward fully organic nano-scale transistors that could be fabricated on any type of substrate. It has also an important impact on performances. Indeed, most CNTFETs suffer from very severe hysteresis in their transfer characteristics (I_D–V_{GS}), which originate principally from trap states in the inorganic dielectric layer and adsorbed molecules at their surface (in particular water). Recently, we showed that a single molecular layer of alkanethiol molecules can be used as an ultra-thin organic dielectric for CNTFETs. The proposed geometry is shown in the insert of Fig. 9. It consists of a single nanotube deposited on top of a thin gold electrode on which a self-assembled monolayer of octadecanethiol has been prepared. The nanotube is connected to the Pd/Au source and drain electrodes in a final stage using a fabrication protocol that preserves the density and organization of the molecular layer. As shown in Fig. 9, no hysteresis is observed in the I_D–V_{GS} characteristics due to the reduced density of trap states in such molecular layer and to its hydrophobic character. More over, the reduced dielectric thickness ($\sim$2.2 nm) leads to an ideal sub-threshold slope of $\sim$60 mV/dec (in the presented example) proving the excellent gate coupling achieved in such configuration [64].

5.2. Opto-electronic nanotube devices

Semiconducting carbon nanotubes have interesting optical properties among which a direct band-gap, the energy of which depends on the nanotube diameter. From 2002, individual nanotubes have been incorporated into several types of optoelectronic devices [65], in particular nano-scale light sources [66] and sensors [67]. Instead of relying on the optical properties of the nanotubes, which vary from one nanotube to the other, one can try to develop opto-electronic devices which combine the exceptional electrical properties of nanotubes with additional optical properties brought in by organic molecules. These molecules can be simply deposited or, better, chemically grafted on the nanotube (see Section 2 and Ref. [5]). A few examples of such strategy have been recently demonstrated [68–70,32,18]. One particularly interesting route for both its simplicity and the originality of the achieved functionality consists in coating a CNTFET with a thin film of a photo-conducting polymer [68,70,18]. We fabricated CNTFETs using the chemical
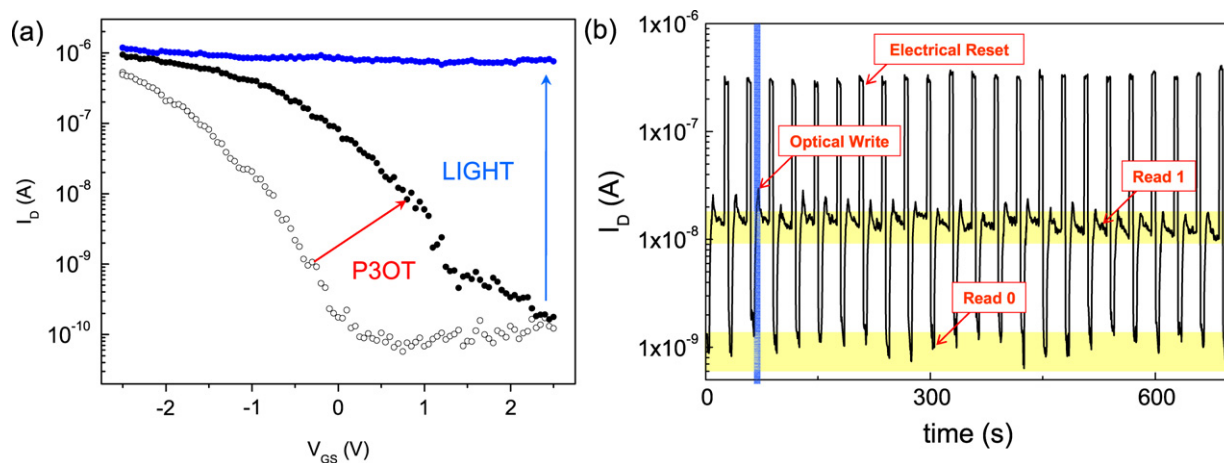
Fig. 10. (a) Transfer characteristics of a nanotube transistor before (open circles) and after (black dots) functionalization by a thin film of P3OT and of the same device under illumination (at $\lambda = 457$ nm, blue dots). At $V_{GS} = 2.5$ V, light induces a four orders of magnitude increase of the nanotube conductivity. (b) $I_D(t)$ plot showing the robustness of the memory effect based on an "optical write–electrical erase" principle: a light pulse (only one blue shaded area is represented for clarity) brings the device in its on-state ('1') and a negative bias pulse at $V_{GS} = -4$ V brings it back to its off-state ('0').

self-assembly technique described above and functionalized them with a thin film ($\sim$5 nm) of poly(3-octyl-thiophene), a semiconducting conjugated polymer. We showed that the photo-generation of charges in the polymer allows the modulation of the nanotube conductivity over four orders of magnitude as presented in Fig. 10(a) [18]. The static and transient electrical properties under illumination, of pristine and functionalized nanotube transistors, as well as organic TFTs without nanotubes were studied. They demonstrated that the optical command of the devices is due to electron trapping at the interface between the gate dielectric and the polymer. Depending on the gate bias, the device behaves as an optically driven current modulator or as an electrically erasable non-volatile optical memory. The programmability and stability of such memory device is illustrated in Fig. 10(b). To confirm the critical impact of the dielectric in this type of devices, we fabricated CNTFETs using TiO_2 as gate dielectric [19]. The comparison of the opto-electronic responses of these devices with their SiO_2-based counterparts (see Fig. 11) allows studying in details the nature and dynamics of charge trapping mechanisms. In this configuration, the carbon nanotube acts as a local probe, remarkably sensitive to the photo-generated charge distribution in the polymer film and at the polymer-dielectric interface, and we proposed to use this probe to study organic–inorganic interfaces that are important in the framework of organic electronics and solar cells [19].

5.3. High frequency carbon nanotube transistors

Semiconducting SWNTs are one of the most promising materials for the development of electronic devices working at very high frequencies. Several theoretical estimations predict cut-off frequencies in the THz range for short channel nanotube transistors in the ballistic regime [71,72]. More detailed models, in particular those developed at the IEF-Orsay in the group of Ph. Dollfus and S. Retailleau, include the impact of phonon scattering and have improved to a point where they become valuable guides for the design of future high frequency devices [59,73,74].

However, despite this high potential, experimental realizations are still sparse and the measured frequencies limited to moderate values. They comes principally from two factors: (i) the high impedance of individual nanotubes ($>$6.5 kΩ) is not adapted to conventional HF equipment (50 Ω); and (ii) the parasitic contributions usually dominate over the intrinsic nanotube contributions due, in particular, to its very small size in comparison to the complete device structure. To overcome these difficulties, several research groups have used strategies based on either mixing techniques [75–77], direct transmission coefficient measurement [78] or multi-channel devices [79].

In close collaboration with the group of G. Dambrine at IEMN (CNRS, Lille), we have developed high frequency carbon nanotube-based devices composed of multiple nanotubes in parallel, which allow a correct matching to 50 Ω and lower the impact of parasitic capacitances. Our first realizations [80,15] were based on random networks of
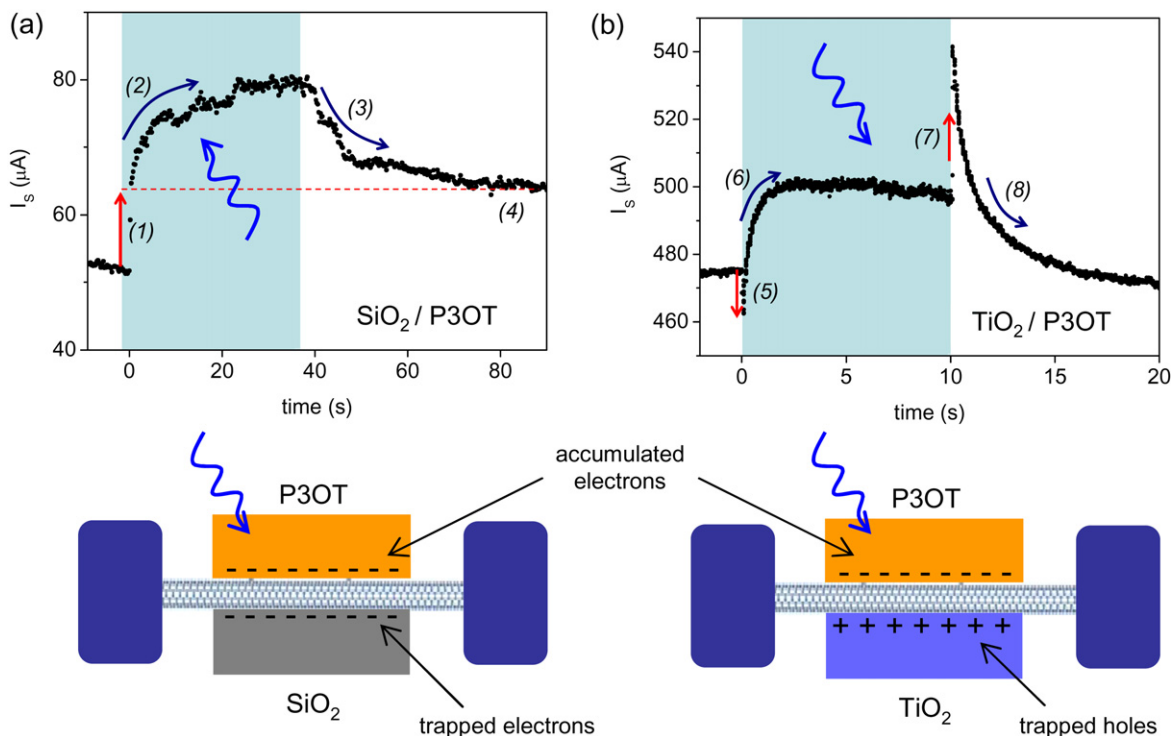
Fig. 11. (a) $I_D(t)$ plot of an OG-CNTFET using SiO_2 as gate dielectric and associated schematics. Illumination at $\lambda = 457$ nm (blue shaded area) results in electron trapping in SiO_2 (1) followed by electron accumulation in the P3OT (2). At light turn off, the charge in the P3OT relaxes (3) while the trapped electrons form the memory state (4). (b) Same for a device made on TiO_2. Light results in holes trapping in TiO_2 (5) followed by electron accumulation in the P3OT (6). At light turn off, part of the charges in the P3OT recombine with charges in the TiO_2 (7) and finally the excess of charge in the P3OT relaxes (8) [19].

nanotubes assembled using surface chemistry (see details on the APTS method above). In such a configuration, we obtained a current gain cut-off frequency (f_T) of 8 GHz (after de-embedding, i.e. correcting the impact of parasitic capacitance using data obtained on similar structures without nanotubes). We recently proposed an improved version of this device using dense networks of preferentially aligned nanotubes. These networks were assembled using the dielectrophoresis technique described above. Nanotubes dispersed in solution are attracted toward the source and drain electrodes using an AC electric field, which drives and aligns the nanotubes. With such 2D film of aligned nanotubes, f_T reaches 30 GHz (after de-embedding) and the transconductance remains constant up to at least 20 GHz [16]. While being the present highest measured f_T for a nanotube-based device, it is still well below the intrinsic potential of nanotubes. Several routes for the improvement of this performance have been identified and are presently investigated.

Interestingly, the methods of fabrication and characterization we used in this study are compatible with any type of substrate, in particular plastics. This opens new opportunities for the realization of high frequency flexible electronic devices. Carbon nanotubes have been identified early as interesting candidates for the development of flexible electronic devices [81–84]. Indeed, they combine the required mechanical flexibility with very high carrier mobility ($>10^4$ cm^2/V s). This last advantage is particularly important when compared with conventional organic electronic materials such as semiconducting polymers, in which the carrier mobility is usually in the 10^{-3}–1 cm^2/V s range. Using the same strategy as for CNT devices on silicon, we recently demonstrated nanotube-based flexible transistors with as-measured f_T as high as 1 GHz [17] and constant transconductance up to 6 GHz, as shown in Fig. 12. We notably showed that the DC transconductance of such devices fabricated on a polyethylenterephtalate substrate remains constant down to radius of curvature of $\sim$3.3 mm, a value already satisfactory for most envisioned flexible electronic applications. Thus, nanotubes prove by far more promising than conventional organic materials and already compete favourably with flexible semiconducting nanowires and ribbons [85–87]. In this context, better performance at strong bending angles are expected due to the superior elasticity of CNTs.
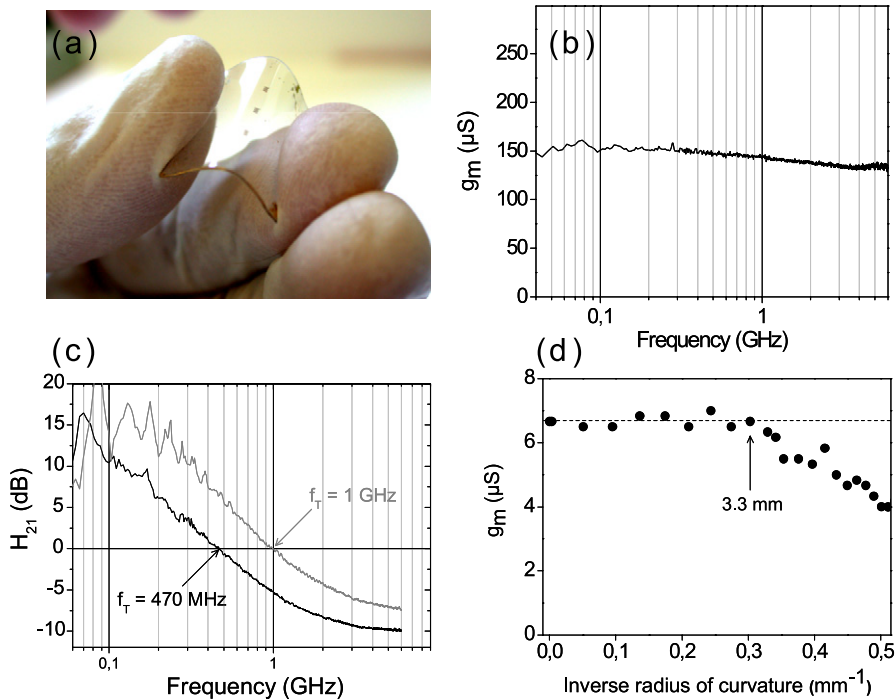
Fig. 12. (a) 3×6 HF nanotube transistors on a polyethylen-terephtalate film (PET) [17]. (b) Frequency evolution of the device transconductance. (c) Frequency evolution of the current gain H_{21} of a typical device (black) and of the best device (gray). The corresponding f_T are 470 MHz and 1 GHz. (d) Evolution of the DC transconductance as a function of bending (unit inverse of the radius of curvature). g_m remains constant down to $\sim$3.3 mm then decreases due to disconnection of nanotubes from the Pd electrodes.

6. Carbon nanotube based Nano-Electro-Mechanical Systems (NEMS)

CNTs are promising candidates for designing and developing nanoelectromechanical systems (NEMS) because they combine excellent electronic and mechanical properties. High conductivity of CNTs allows for designing simple sensing and actuation systems based on the direct electrostatic coupling with metallic gates. Their exceptional stiffness, low mass and dimensions ensure operating frequencies in the GHz range making them suitable for a number of applications [88]. The aim of our activity in this field is to explore the relevance of carbon nanotubes in NEMS applications. The first step towards this goal is to understand the electromechanical properties of CNTs. We performed numerical calculations on simple structures comprising a single CNT. The heart of the system is a doubly clamped suspended CNT three-terminal device (see insert of Fig. 13(b)) deflected by an electrostatic force induced by a back gate voltage V_G. Numerical calculations of the maximum deflection u of the CNT as a function of the gate voltage V_G for various diameters D and lengths L of the CNT show that a scaling law linking u to V_G exists for a fixed CNT-gate distance. Indeed, all the curves $u(V_G)$ are superimposed when plotting u/D as a function of a normalized gate voltage $V_G L^2 D^{-2.25}$ [20]. This scaling law derived from continuum beam theory when $u_{MAX} \ll D$, is observed in the whole bias range and allows one to finely adjust the geometry of each device. The discovery of this scaling law motivated the realization of an experiment intended to validate it in the simplest way. For this experiment we fabricated a structure comprising a suspended CNT connected to two metal electrodes. The gate (heavily doped silicon) is used to attract the CNT electrostatically. The tip of an atomic force microscope (AFM), placed at the center of the CNT is used to detect the vertical deflection u. Measurements of u as a function of the gate voltage V_G for different NTs (different D and L) show clearly and without adjustable parameters the existence of such a scaling law (Fig. 13(a)–(b)). These results allow us to obtain the Young modulus of the CNTs used (ca 0.4 TPa) [20].

The work now targets the measurement of the dynamical (high frequency) properties of CNT based NEMS. In order to correlate static and high frequency measurements, a modified AFM setup was implemented following Ref. [89]. Fig. 13(c) shows preliminary results [90] on a MWNT-NEMS device ($D = 6$ nm and $L = 600$ nm). Two peaks are observed at 102 and 204 MHz respectively. Since the gate excitation applied is $V = V_{dc} + V_{ac} \cos(2\pi f_t)$ with
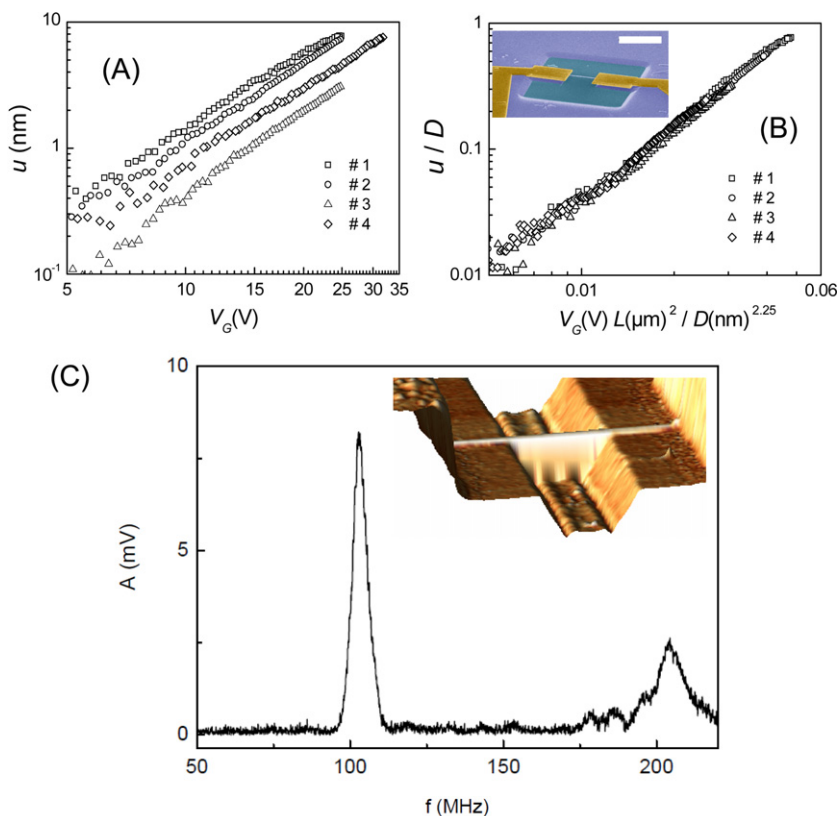
Fig. 13. (A) Maximum deflection u as a function of V_G for devices #1 ($L = 600$ nm, $D = 10$ nm), #2 ($L = 770$ nm, $D = 13.5$ nm), #3 ($L = 480$ nm, $D = 10$ nm) and #4 ($L = 975$ nm, $D = 21.5$ nm). (B) Normalized u as a function of rescaled V_G. Insert: SEM image of a typical device used in AFM experiments. (C) Resonant signal as a function of frequency measured by AFM [90] using the experimental method described in Ref. [89]. Insert: AFM image of the suspended MWNT.

$V_{dc} \sim V_{ac}$, the observed signal corresponds to the same mechanical resonance with a resonant frequency equal to 204 MHz. This value is consistent with a Young's modulus of 0.43 TPa in agreement with what was obtained in static measurements on the same MWNT source. Furthermore, the obtained value implies that the built-in mechanical stress in the case of MWNT is negligible.

The understanding of the electromechanical behaviour of CNTs and the developed know-how in fabricating CNT-based devices led us to realize suspended switches based on individual CNTs [21]. The fabrication process consists in preparing a trench by reactive ion etching through a mask deposited on a silicon substrate and then to fill it by metal evaporation up to a chosen thickness thus leaving a well defined gap (precision of 2 nm) between the upper surface of the metal electrode and the substrate surface. Multiwalled NTs are then deposited perpendicular to the buried electrode by the chemical self-assembly technique described above. NTs are then connected electrically by evaporation of metal contacts (Fig. 14(a)). In this geometry, where the distance between the nanotube and the metal electrode is small, the deformation of the nanotube brings it in contact with the electrode, giving rise to a very effective switch behaviour due to the mechanical instability appearing beyond a threshold deformation (corresponding approximately to the third of CNT-electrode initial distance). Once in contact with the electrode, the van der Waals interaction keeps the CNT stuck even under reduced bias (Fig. 14(b)). The competition between this van der Waals interaction and the mechanical force can be fine tuned by adjusting the CNT diameter, suspension length and initial gap size, so that both efficient switches or memory devices can be targeted [91].

7. Conclusion

In this review of our recent results, we showed that carbon nanotubes handled in solution can lead to the development of innovative electronic devices with remarkable functionality and performance. These devices result from
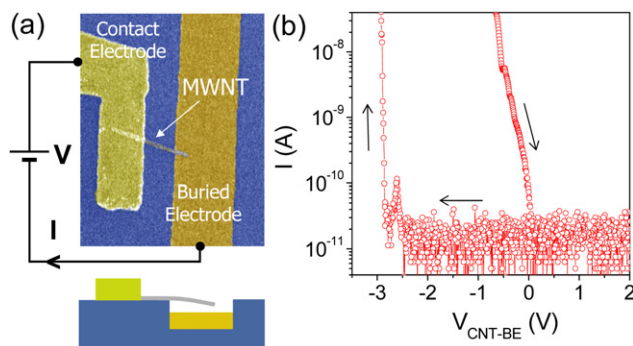
Fig. 14. (a) SEM image of a singly clamped MWNT in cantilever geometry. (b) $I(V)$ characteristics of the electromechanical switch. From $V = 0$ to -2.9 V, the MWNT is attracted toward the bottom electrode but no current is detected. At -2.9 V, the CNTs experience a mechanical instability and jump into contact, leading to a sharp increase in current [21].

the combined use of chemical functionalization and self-assembly techniques that are the basis of our approach. We also showed that advanced theoretical work can help predicting the complex and critical impact of nanotube functionalization. These types of calculations become central tools both to understand in depth and guide device oriented studies. With the ever improving quality of the available SWNTs sources and the development of new purification and sorting methods, SWNTs become serious candidates to target specific applications, in particular in the field of large scale, flexible electronics. In addition, the better control of individual devices opens new routes for the development of circuit architectures for the efficient exploitation of nano-devices. This represents an important direction of our present nanotube activity.

Acknowledgements

References

[1] D. Tasis, N. Tagmatarchis N, A. Bianco, M. Prato, Chem. Rev. 106 (2006) 1105–1136.
[2] M. Hersam, Nature Nanotechnology 3 (2008) 387–394.
[3] L. Capes, E. Valentin, S. Esnouf, A. Ribayrol, O. Jost, A. Filoramo, J.N. Patillon, Proc. IEEE Conf. on Nanotechnology, 2002, pp. 439–442.
[4] G. Schmidt, S. Gallon, S. Esnouf, J.-P. Bourgoin, P. Chenevier, Chem. Eur. J. 15 (2009) 2101.
[5] S. Campidelli, B. Ballesteros, A. Filoramo, D. Díaz Díaz, G. de la Torre, T. Torres, G.M.A. Rahman, C. Ehli, D. Kiessling, F. Werner, V. Sgobba, D.M. Guldi, C. Cioffi, M. Prato, J.-P. Bourgoin, J. Am. Chem. Soc. 130 (2008) 11503.
[6] K.H. Choi, J.-P. Bourgoin, S. Auvray, D. Estève, G.S. Duesberg, S. Roth, M. Burghard, Surf. Sci. 472 (2000) 195.
[7] E. Valentin, S. Auvray, J. Goethals, J. Lewenstein, L. Capes, A. Filoramo, A. Ribayrol, R. Tsui, J.-P. Bourgoin, J.-N. Patillon, Microelect. Eng. 61 (2002) 491–496.
[8] E. Valentin, S. Auvray, A. Filoramo, A. Ribayrol, M.F. Goffman, L. Capes, J.-P. Bourgoin, J.-N. Patillon, Proc. MRS Symp. 772 (2003) 201–207.
[9] E. Valentin, S. Auvray, A. Filoramo, A. Ribayrol, M.F. Goffman, J. Goethals, L. Capes, J.-P. Bourgoin, J.-N. Patillon, in: A.S. Alexandrov, J. Demsar, I.K. Yanson (Eds.), Proc. of the NATO Advanced Research Workshop on Molecular Nanowires and Other Quantum Objects, in: NATO Science Series II, vol. 148, Springer-Verlag, Berlin, 2004, p. 57.
[10] C.-L. Chung, K. Nguyen, S. Lyonnais, S. Streiff, S. Campidelli, L. Goux-Capes, J.-P. Bourgoin, A. Filoramo, AIP Proc. of the Int. Symp. on DNA-Based Nanodevices, Jena, Germany, 29–31 May 2008, ISBN: 978-0-7354-0592-9.
[11] S. Lyonnais, L. Goux-Capes, C. Escudé, D. Cote, A. Filoramo, J.-P. Bourgoin, Small 4 (2008) 442.

[12] S. Lyonnais, C.-L. Chung, L. Goux-Capes, C. Escudé, O. Piétrement, S. Baconnais, E. Le Cam, J.-P. Bourgoin, A. Filoramo, Chem. Commun. (2009) 683.
[13] S. Auvray, J. Borghetti, M.F. Goffman, A. Filoramo, V. Derycke, J.P. Bourgoin, O. Jost, Appl. Phys. Lett. 84 (2004) 5106–5108.
[14] S. Auvray, A. Filoramo, M.F. Goffman, V. Derycke, O. Jost, J.P. Bourgoin, Nano Lett. 5 (2005) 451.
[15] J.-M. Bethoux, H. Happy, G. Dambrine, V. Derycke, M.F. Goffman, J.-P. Bourgoin, IEEE Electron Device Lett. 27 (2006) 681–683.
[16] A. Le Louarn, F. Kapche, J.-M. Bethoux, H. Happy, G. Dambrine, V. Derycke, P. Chenevier, N. Izard, M.F. Goffman, J.-P. Bourgoin, Appl. Phys. Lett. 90 (2007) 233108.
[17] N. Chimot, V. Derycke, M.F. Goffman, J.P. Bourgoin, H. Happy, G. Dambrine, Appl. Phys. Lett. 91 (1) (2007) 53111.
[18] J. Borghetti, V. Derycke, S. Lenfant, P. Chenevier, A. Filoramo, M.F. Goffman, D. Vuillaume, J.-P. Bourgoin, Adv. Mater. 18 (2006) 2535–2540.
[19] C. Anghel, V. Derycke, A. Filoramo, S. Lenfant, B. Giffard, D. Vuillaume, J.P. Bourgoin, Nano Lett. 8 (2008) 3619.
[20] R. Lefèvre, M.F. Goffman, V. Derycke, C. Miko, L. Forró, J.-P. Bourgoin, P. Hesto, Phys. Rev. Lett. 95 (2005) 185504.
[21] E. Dujardin, V. Derycke, M.F. Goffman, R. Lefèvre, J.-P. Bourgoin, Appl. Phys. Lett. 87 (2005) 193107.
[22] A. Lopez Bezanilla, F. Triozon, S. Latil, X. Blase, S. Roche, Nano Lett. 9 (2009) 940.
[23] H.C. Kolb, M.G. Finn, K.B. Sharpless, Angew. Chem. Int. Ed. 40 (2001) 2004.
[24] R. Huisgen, in: A. Padwa (Ed.), 1,3-dipolar Cycloaddition Chemistry, Wiley, New York, 1984, p. 1.
[25] V.V. Rostovtsev, L.G. Green, V.V. Fokin, K.B. Sharpless, Angew. Chem. Int. Ed. 41 (2002) 2596.
[26] C.W. Tornøe, C. Christensen, M. Meldal, J. Org. Chem. 67 (2002) 3057.
[27] V.D. Bock, H. Hiemstra, J.H. van Maarseveen, Eur. J. Org. Chem. 1 (2006) 51–68.
[28] H. Li, F. Cheng, A.M. Duft, A. Adronov, J. Am. Chem. Soc. 127 (2005) 14518.
[29] Z. Guo, L. Liang, J.-J. Liang, Y.-F. Ma, X.-Y. Yang, D.-M. Ren, Y.-S. Chen, J.-Y. Zheng, J. Nanopart. Res. 10 (2008) 1077.
[30] B.L. Allen, P.D. Kichambare, A. Star, Adv. Mater. 19 (2007) 1439.
[31] B. Ballesteros, S. Campidelli, G. de la Torre, C. Ehli, D. Guldi, M. Prato, T. Torres, Chem. Commun. 28 (2007) 2950–2952.
[32] J.M. Simmons, I. In, V.E. Campbell, T.J. Mark, F. Léonard, P. Gopalan, M.A. Eriksson, Phys. Rev. Lett. 98 (2007) 086802.
[33] K. Balasubramanian, E.J.H. Lee, R.T. Weitz, M. Burghard, K. Kern, Phys. Status Solidi A 205 (2008) 633.
[34] S. Latil, S. Roche, J.-C. Charlier, Nano Lett. 5 (2005) 2216.
[35] F. Tournus, S. Latil, M.I. Heggie, J.-C. Charlier, Phys. Rev. B 72 (2005) 075431.
[36] J. Zhao, H. Park, J. Han, J. Lu, J. Phys. Chem. B 108 (2004) 4227.
[37] H. Park, Z. Zhao, J.P. Lu, Nanotechnology 16 (2005) 635.
[38] J. Cabana, R. Martel, J. Am. Chem. Soc. 129 (2007) 2244.
[39] M.B. Nardelli, Phys. Rev. B 60 (1999) 7828.
[40] Y.-S. Lee, M. Buongiorno Nardelli, N. Marzari, Phys. Rev. Lett. 95 (2005) 076804.
[41] Y.-S. Lee, N. Marzari, Phys. Rev. Lett. 97 (2006) 116801.
[42] J. Liu, et al., Chem. Phys. Lett. 303 (1999) 125.
[43] J. Muster, et al., J. Vac, Sci. Tech. B 16 (1998) 2796.
[44] R. Krupke, F. Hennrich, H. von Lohneysen, M.M. Kappes, Science 301 (2003) 344–347.
[45] N.C. Seeman, Nature 421 (2003) 427.
[46] J. Richter, Physica E 16 (2003) 157.
[47] K. Nguyen, M. Monteverde, A. Filoramo, L. Goux-Capes, S. Lyonnais, P. Jegou, P. Viel, M. Goffman, J.-P. Bourgoin, Adv. Mater. 20 (2008) 1099.
[48] S.J. Tans, A.R.M. Verschueren, C. Dekker, Nature 393 (1998) 49.
[49] R. Martel, T. Schmidt, H.R. Shea, T. Hertel, P. Avouris, Appl. Phys. Lett. 73 (1998) 2447.
[50] J.C. Charlier, X. Blase, S. Roche, Rev. Mod. Phys. 79 (2007) 677.
[51] A. Javey, J. Guo, D.B. Farmer, Q. Wang, E. Yenilmez, R.G. Gordon, M. Lundstrom, H. Dai, Nano Lett. 4 (2004) 1319.
[52] R.V. Seidel, A.P. Graham, J. Kretz, B. Rajasekharan, G.S. Duesberg, M. Liebau, E. Unger, F. Kreupl, W. Hoenlein, Nano Lett. 5 (2005) 147.
[53] A. Javey, P. Qi, Q. Wang, H. Dai, Proc. Natl. Acad. Sci. USA 101 (2004) 13408.
[54] Y.M. Lin, J. Appenzeller, Z.H. Chen, Z.G. Chen, H.M. Cheng, P. Avouris, IEEE Elec. Dev. Lett. 26 (2005) 823.
[55] J. Kong, N.R. Franklin, C.W. Zhou, M.G. Chapline, S. Peng, K.J. Cho, H.J. Dai, Science 287 (2000) 622.
[56] K. Besteman, J.O. Lee, F.G.M. Wiertz, H.A. Heering, C. Dekker, Nano Lett. 3 (2003) 727.
[57] A. Javey, J. Guo, Q. Wang, M. Lundstrom, H. Dai, Nature 424 (2003) 6949.
[58] Z.H. Chen, J. Appenzeller, J. Knoch, Y.M. Lin, P. Avouris, Nano Lett. 5 (2005) 1497.
[59] H. Cazin d'Honincthun, S. Galdin-Retailleau, A. Bournel, Ph. Dollfus, J.-P. Bourgoin, C. R. Physique 9 (2008) 67–77.
[60] R. Martel, V. Derycke, C. Lavoie, J. Appenzeller, K. Chen, J. Tersoff, Ph. Avouris, Phys. Rev. Lett. 87 (2001) 256805.
[61] J. Appenzeller, J. Knoch, V. Derycke, R. Martel, S. Wind, P. Avouris, Phys. Rev. Lett. 89 (2002) 126801.
[62] S.-H. Hur, M.-H. Yoon, A. Gaur, M. Shim, A. Facchetti, T.J. Marks, J.A. Rogers, J. Am. Chem. Soc. 127 (2005) 13808.
[63] R.T. Weitz, U. Zschieschang, F. Effenberger, H. Klauk, M. Burghard, K. Kern, Nano Lett. 7 (2007) 22–27.
[64] G. Robert, V. Derycke, M.F. Goffman, S. Lenfant, D. Vuillaume, J.-P. Bourgoin, Appl. Phys. Lett. 93 (2008) 143117.
[65] P. Avouris, M. Freitag, V. Perebeinos, Top. Appl. Phys. 111 (2008) 423.
[66] J.A. Misewich, R. Martel, P. Avouris, J.C. Tsang, S. Heinze, J. Tersoff, Science 300 (2003) 783.
[67] M. Freitag, Y. Martin, J.A. Misewich, R. Martel, P. Avouris, Nano Lett. 3 (2003) 1067.
[68] A. Star, Y. Lu, K. Bradley, G. Gruner, Nano Lett. 4 (2004) 1587.
[69] X. Guo, L. Huang, S. O'Brien, P. Kim, C. Nuckolls, J. Am. Chem. Soc. 127 (2005) 15045.

[70] K.S. Narayan, M. Rao, R. Zhang, P. Maniar, Appl. Phys. Lett. 88 (2006) 243507.

[71] P.J. Burke, Solid-State Electron. 48 (2004) 1981.

[72] Lundstrom, et al., IEEE Trans. Nanotechnol. 4 (2005) 1536.

[73] H. Cazin d'Honincthun, H.N. Nguyen, S. Galdin-Retailleau, et al., Physica E: Low Dim. Sys. & Nanostruct. 40 (2008) 2294–2298.

[74] S. Fregonese, H. Cazin d'Honincthun, J. Goguet, et al., IEEE Trans. Elec. Dev. 55 (2008) 1317.

[75] J. Appenzeller, D.J. Frank, Appl. Phys. Lett. 84 (2004) 1771.

[76] S. Rosenblatt, H. Lin, V. Sazonova, S. Tiwari, P.L. McEuen, Appl. Phys. Lett. 87 (2005) 153111.

[77] A.A. Pesetski, J.E. Baumgardner, E. Folk, J.X. Przybysz, J.D. Adam, H. Zhang, Appl. Phys. Lett. 88 (2006) 113103.

[78] J. Chaste, L. Lechner, P. Morfin, G. Feve, T. Kontos, J.M. Berroir, D.C. Glattli, H. Happy, P. Hakonen, B. Placais, Nano Lett. 8 (2008) 525–528.

[79] D. Wang, Z. Yu, S. McKernan, P.J. Burke, IEEE Trans. Nanotechnol. 6 (2007) 400–403.

[80] J.-M. Bethoux, H. Happy, A. Siligaris, G. Dambrine, J. Borghetti, V. Derycke, J.-P. Bourgoin, IEEE Trans. Nanotechnol. 5 (2006) 335.

[81] K. Bradley, J.C.P. Gabriel, G. Gruner, Nano Lett. 3 (2003) 1353.

[82] E. Artukovic, M. Kaempgen, D.S. Hecht, S. Roth, G. Gruner, Nano Lett. 5 (2005) 757.

[83] Q. Cao, S.H. Hur, Z.T. Zhu, Y. Sun, C. Wang, M.A. Meitl, M. Shim, J.A. Rogers, Adv. Mater. 18 (2006) 304.

[84] S.J. Kang, C. Kocabas, T. Ozel, M. Shim, N. Pimparkar, M.A. Alam, S.V. Rotkin, J.A. Rogers, Nat. Nanotechnol. 2 (2007) 230.

[85] H.C. Yuan, Z. Ma, Appl. Phys. Lett. 89 (2006) 212105.

[86] J.H. Ahn, H.S. Kim, K.J. Lee, Z. Zhu, E. Menard, R.G. Nuzzo, J.A. Rogers, IEEE Electron. Dev. Lett. 27 (2006) 460.

[87] Y. Sun, E. Menard, J.A. Rogers, H.S. Kim, S. Kim, G. Chen, I. Adesida, R. Dettmer, R. Cortez, A. Tewksbury, Appl. Phys. Lett. 88 (2006) 183509.

[88] A.N. Cleland, Foundations of Nanomechanics, Springer-Verlag, Berlin, 2003.

[89] D. Garcia-Sanchez, et al., Phys. Rev. Lett. 99 (2007) 085501.

[90] M.F. Goffman, N. Chimot, E. Mile, M.C. Monteverde, J.-P. Bourgoin, V. Derycke, Proc. SPIE 7037 (2008) 703702.

[91] L.M. Jonsson, T. Nord, J.M. Kinaret, S. Viefers, J. Appl. Phys. 96 (2004) 629.